Exploitation of S-Layer Anisotropy: pH-Dependent Nanolayer Orientation for Cellular Micropatterning

Mario Rothbauer,[†] Seta Küpcü,[‡,*] Drago Sticker,[†] Uwe B. Sleytr,[§] and Peter Ertl[†]

[§]Institute for Biophysics, Department of Nanobiotechnology, [‡]Institute for Synthetic Bioarchitectures, Department of Nanobiotechnology, [†]BioSensor Technologies, Austrian Institute of Technology (AIT), University of Natural Resources and Life Science, Muthgasse 11, Vienna 1190, Austria

ABSTRACT We have developed a tunable, facile, and reliable cell patterning method using a self-assembled crystalline protein monolayer that, depending on its orientation, can exhibit either cell adhesive (cytophilic) or cell repulsive (cytophobic) surface properties. Our technique exploits, for the first time, the inherent biological anisotropy of the bacterial cell wall protein SbpA capable of interacting with its cytophilic inner side with components of the cell wall, while its outer cytophobic side interacts with the environment. By simply altering the recrystallization protocol from a basic to an acidic condition, the SbpA-protein layer orientation and function can be switched from preventing unspecific protein adsorption and cell adhesion to effectively promote cell attachment, spreading, and proliferation. As a result, the same protein solution can be used to form cell adhesive and repulsive regions over large areas on a single substrate using a simple pH-dependent self-assembly procedure. The reliable establishment of cytophobic and cytophilic SbpA layers allows the generation of well-defined surface patterns that exhibit uniform height (9−10 nm), p4 lattice symmetry with center-to-center spacing of the morphological units of 12 nm, as well as similar surface potential and charge distributions under cell culture conditions. The pH-dependent "orientation switch" of the SbpA protein nanolayer was integrated with micromolding in capillaries (MIMIC) technology to demonstrate its application for cell patterning using a variety of cell lines including epithelial, fibroblast and endothelial cells.

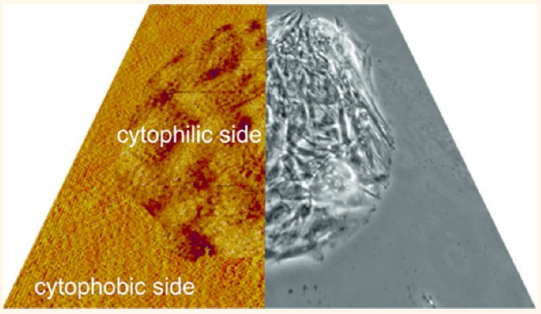

KEYWORDS: S-layer · SbpA · cell patterning · self-assembly · micromolding in capillaries

It is well established that the spatial organization of cells within a tissue impacts cellular activity, which in turn influences tissue function. Since the spatial arrangement of cells in their microenvironment controls cell behavior, controlling the spatial organization of cells is highly relevant to *in vitro* cell culture methods. A variety of surface patterning strategies for cell cultures have been developed to mimic the *in vivo* cellular microenvironment.[1] In this regard, the fabrication of micropatterned surfaces is an indispensable tool in cell biology in terms of influencing and controlling cellular functions such as cell adhesion, migration, proliferation, cell shape, and apoptosis, as well as cell differentiation and distinct lineage commitment.[2,3] One crucial aspect of regulating cell behavior using specific surface topographies and chemistries relates to using patterned surfaces similar to the extracellular matrix (ECM) *in situ* in terms of size and scale. This means that patterned surfaces have to influence cells at the nano- and microscale. It has been shown that cells react to nanoscale surface signals of approximately 10 nm spatial resolution, which corresponds to ECM features found *in vivo*.[4] Alternatively, directed cell orientation and migration is observed by introducing larger microscale structures including ridges, fibers, and grooves.[5,6] Interaction between cells and the patterned surface at both nano- and microscale induce cytoskeletal changes in cells, including the reorientation of actin filaments and microtubules as well as the localization of focal adhesion proteins.[7−9]

Various technologies exist to generate the desired surface features including photolithography, soft lithography, plasma lithography, microcontact printing (μCP), and microfluidic surface structuring.[10−19] Independent of the surface structuring method employed, a common strategy concerning cell patterning includes the precise

* Address corresponding to seta.küpcü@boku.ac.at.

Received for review June 24, 2013 and accepted August 29, 2013.

Published online August 29, 2013
10.1021/nn403198a

positioning of cell repulsive (cytophobic) and cell adhesive (cytophilic) areas to modulate cell behavior. Cytophobic and cytophilic surfaces are created using metal thin films, polymers, self-assembled monolayers (SAMs), ECM proteins, cell-adhesion peptides, and bioactive molecules. The disadvantage of using thin film and polymer-based patterns is that these biologically foreign surfaces may induce nonphysiological cell responses.[20] SAMs with tailored hydrophobic and hydrophilic surface properties, however, can be used to better control the chemistry and composition of micropatterned surfaces to influence protein adsorption and cell adhesion.[21] Nevertheless, the drawback of using SAMs is that the surface fabrication process is complex and tedious, with multiple patterning procedures that require an additional functionalization step to attach specific cell-adhesion promoters.[22] Although protein-based strategies that rely on physisorption of cell-adhesive ECM components such as fibronectin, collagen, and laminin have become the method of choice for cellular patterning, a variety of shortcomings still persist.[23,24] For instance, the generation of cytophilic protein patterns involving the colocalization of cytophobic areas that effectively inhibit protein adsorption is often difficult to achieve. Furthermore, the stability of a variety of protein-based patterns and their resistance to cellular degradation is often not sufficient for long-term cell culture applications. One strategy shown to overcome some of these drawbacks is the application of the fungal protein hydrophobin, which can undergo controlled self-assembly and can therefore change the physicochemical properties of a cell repulsive surface. For instance, the growth of adherent cells on hydrophobic surfaces such as Teflon was accomplished by patterning a genetically engineered RGD-peptide carrying a hydrophobin fusion-protein.[25]

In this work we introduce a tunable, facile, and reliable cell patterning method based on the controlled orientation of the self-assembled crystalline bacterial surface protein SbpA monolayer that either exhibits cell adhesive (cytophilic) or cell repulsive (cytophobic) surface features. The SbpA protein belongs to a broad class of bacterial surface proteins (S-layers) that represent the outermost cell wall component and perform a variety of important functions, such as acting as precise molecular sieves, providing heat resistance by increasing membrane stability and regulating cell–surface interactions.[26,27] Crystallized protein monolayers are formed at the bacterial cell wall by self-assembly and represent a supramolecular cell envelope structure that features pores identical in size and morphology in the 2–8 nm range, which can be considered as isoporous ultrafiltration membranes.[28,29] At the bacterial cell wall, the inner surface of the S-layer is connected to the secondary cell wall polymer (SCWP), while the outer monolayer surface interacts with the microenvironment.[30,31] The inherent anisotropy of the S-layer is explained by its differing biological functions, including association (inner monolayer surface) to the bacterial cell wall and protective function (outer monolayer surface).[32,33] An advantage of employing S-layers for surface structuring is that they can be readily isolated from the bacterial cell wall using chaotropic agents while maintaining their ability to reattach as well as self-assemble in sheets and cylinders under controlled recrystallization conditions in solution.[34–37] Because the repetitive feature of the S-layer lattice structure aligns functional groups in well-defined positions and orientations at any surface, they have already been used to manipulate material properties including physical and chemical reactivity, porosity, roughness or surface charge, and charge density.[38–41] For instance, the intrinsic antifouling (cytophobic) characteristics of the bacterial surface protein SbpA isolated from Gram-positive mesophilic bacterium *Lysinibacillus sphaericus* CCM 2177 was employed for S-layer ultrafiltration membranes (SUMs).[42]

Our SbpA protein-based micropatterning strategy combines controlled S-layer orientation with micromolding in capillaries (MIMIC) technology to generate single-protein layers on conventional microscope slides. We have exploited, for the first time, the unique biological anisotropy of the SbpA S-layer protein to rapidly generate reliable and reproducible surface patterns that exhibit either cytophobic or cytophilic properties. This means that the same protein solution can be used to form cell adhesive and repulsive regions over large areas on a single substrate using a simple two-step self-assembly procedure. Our SbpA-based micropatterning method allows the generation of chemically well-defined protein monolayers without introducing toxic chemicals, activators and cross-linking agents, thus further increasing the biocompatibility of the cytophilic surface. In this study, pH-dependent SbpA recrystallization was used to control orientation of the SbpA protein layer on glass supports to form smooth cytophobic or rough cytophilic surface patterns. While transmission electron microscopy (TEM) was employed to visualize the outer smooth and inner rough side of the crystallized SbpA-protein layers, atomic force microscopy (AFM), contact angle, and zeta potential measurements were conducted to verify the pH-dependent orientation of the crystallized SbpA nanolayers. Additionally, protein adsorption, cell attachment, and biocompatibility studies using surface plasmon resonance (SPR), electric impedance spectroscopy (EIS), and optical imaging was performed to investigate dynamic cell–surface interactions of normal human dermal fibroblasts (NHDF). Final performance evaluation of our SbpA protein-based surface modification method and its practical application for cell patterning using MIMIC technology is demonstrated using a variety of mammalian cells including

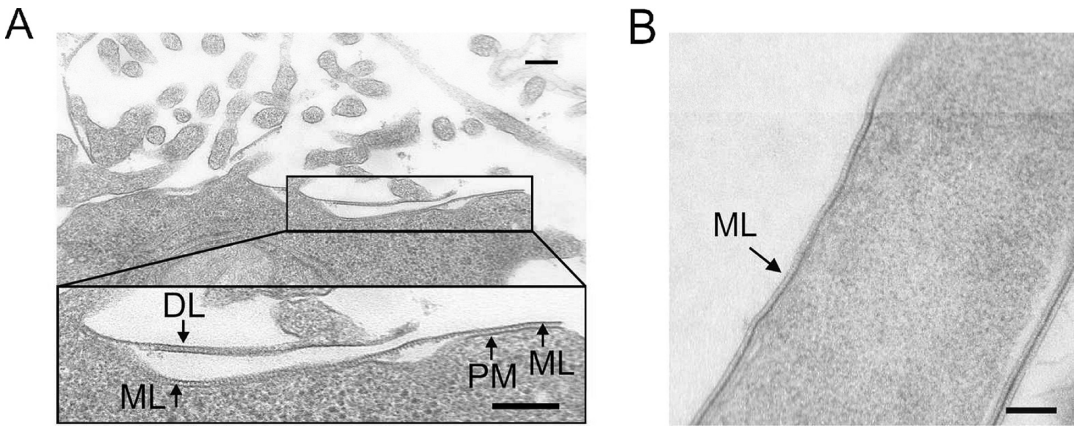

Figure 1. Electron micrographs of ultrathin-section preparations: (A) Interaction of SbpA nanolayers with HepG2 cells. Inlay highlights the interaction of monolayers (ML) with the cell's plasma membrane (PM), whereas no interaction was observable for SbpA doublelayers (DL). (B) Cytophobic, smooth outer surface of SbpA occurring as monolayer (ML) on the bacterial cell wall of Lysinibacillus sphaericus CCM 2177. Bars, 1 μm.

epithelial cells (HeLa, CaCo-2), fibroblasts (NHDF, SMC), and endothelial cells (HUVEC).

RESULTS AND DISCUSSION

Biological Anisotropy of Crystalline SbpA Nanolayers. The key feature of the developed cell patterning method is based on the controlled orientation of the self-assembled crystalline bacterial surface protein SbpA that exhibits either cytophilic or cytophobic surface features. Figure 1A shows the *in vitro* interaction of SbpA self-assembly products with human liver cell (HepG2) cultures. TEM images revealed that SbpA sheets contain mono- as well as bilayer structures that interact differently with the cell surface. Additional experimentation indicates that anchorage-dependent mammalian cell cultures preferentially interact with the rough side of the SbpA monolayer. It is important to note that the SbpA monolayer orientation at the mammalian cell membrane is similar to the orientation of native SbpA formed at the bacterial cell wall (Figure 1B). These results indicate that the rough surface of the SbpA monolayer is associated with the mammalian cell membrane, while the smooth outer surface that interacts with the external environment maintains cytophobic characteristics.

To eventually perform cell patterning, it was important to study assembly efficiency and S-layer orientation on top of a large solid glass surface. Surface topography and physicochemical properties of recrystallized SbpA nanolayers were characterized using AFM, contact angle, and zeta-potential measurements. AFM results shown in Figure 2A demonstrated similar surface topography as reported for other *in vitro* and *in vivo* observations consisting of square p4 lattice symmetry with identical lattice parameters ($a = b =$ 13 nm, $\gamma = 90°$). Monolayer thickness of 10.06 $\pm$ 0.39 nm was further identified using an AFM scratch assay. Additional surface characterization included zeta-potential measurements to compare surface

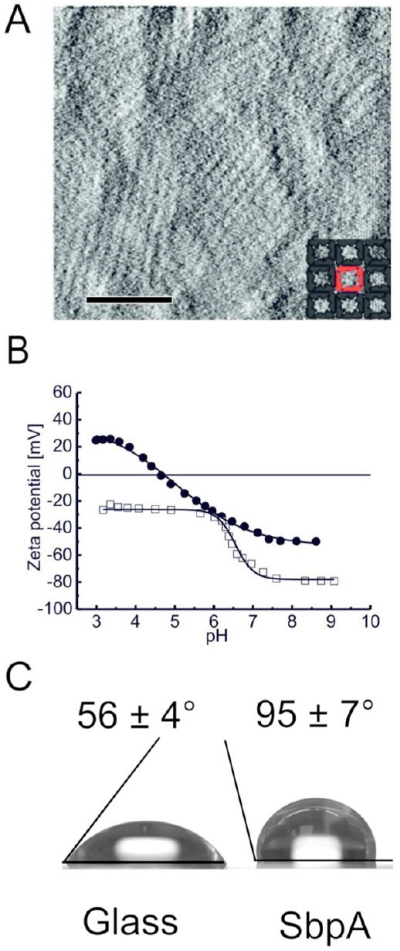

Figure 2. (A) AFM image (deflection mode) showing the topography of the square S-layer protein lattice of SbpA recrystallized on glass (top). The inlay shows a schematic representation of the p4 lattice with one morphological unit highlighted in red. Bar, 100 nm. (B) Zeta potential of protein monolayers of SbpA recrystallized on glass (●) and uncoated glass (□) at pH ranging from 3 to 9. (C) Surface wettability of glass and glass coated with SbpA by measurement of the contact angle of water.

properties between the unmodified glass and the recrystallized SbpA monolayer. Surface potential was

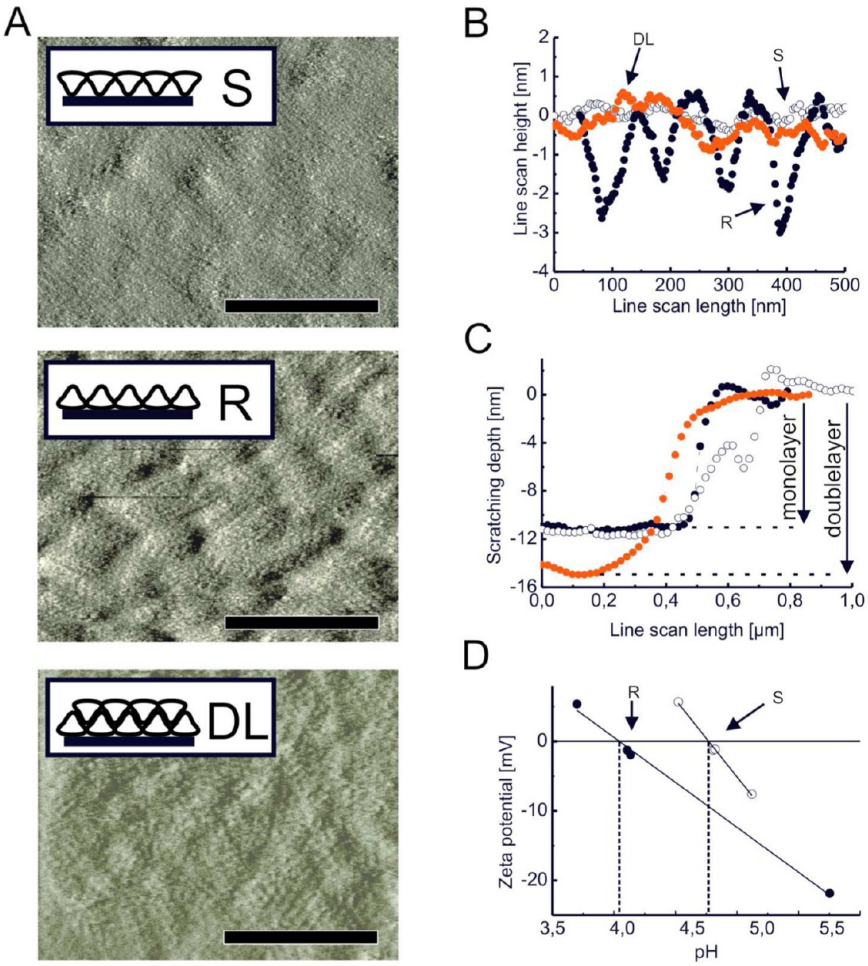

Figure 3. (A) Representative AFM topographs (deflection mode) of SbpA recrystallizations at pH 9 (top image) for smooth (S) monolayers, at pH 4 (center image) for rough (R) monolayers, and of double layers (DL) of SbpA fabricated using a layer-by-layer recrystallization approach (bottom image). Representative AFM line scans for surface roughness (B) and scratching height profiles (C) of SbpA protein monolayers recrystallized at pH 9 (○), pH 4 (●), and of SbpA protein bilayers constructed at pH 4 and pH 9 (orange circle). (D) Streaming potential measurements at a pH range of 3.6 to 5.6 of SbpA protein monolayers after recrystallization on glass at pH 9 (○) and pH 3 (●), demonstrated the shift of IEP from 4.6 to more acidic pH value of 4.0. Bars, 200 nm.

analyzed by pH titration at a range of pH 9.0 to 3.0, as shown in Figure 2B. In comparison to the untreated glass surface having a surface potential of −26 mV at pH 3 and −78 mV at pH 9.0, the titration curve of the SbpA monolayers revealed a surface potential of +25 mV at pH 3 and −50 mV at pH 9.0, confirming that surface modification was successful. Further, the measured isoelectric point (IEP) of approximately pH 4.6 for SbpA corresponds well with calculated IEP from the protein's amino acid sequence (pH 4.7). The SbpA protein monolayer remained stable over the entire pH range and exhibited a net-negative surface charge of −50 mV at the physiologically relevant pH of 7.5. Final contact angle measurements shown in Figure 2C demonstrated a significant increase in hydrophobicity resulting in a contact angle shift from $\theta = 56 \pm 4°$ to $\theta = 95 \pm 7°$ in the presence of crystalline SbpA monolayers. The observed decrease in surface wettability can be associated with the cytophobic outer surface of the SbpA monolayer (see also Figure 1), because similar contact angles are also found on other antifouling materials, such as Teflon.[43] Visual inspection of cell-adhesion using HepG2 cells cultured on partially SbpA modified glass surfaces confirmed the cytophobic properties (no cell attachment observed) of the self-assembled SbpA monolayer on conventional glass surfaces. These results indicate that under the applied self-assembly conditions predominantly a SbpA monolayer is formed on untreated glass surfaces that is oriented with its smooth, cytophobic outer side toward the solution interface.

S-Layer Anisotropy and pH-Dependent Orientation of SbpA Protein Monolayers. The controlled orientation of the cytophilic and cytophobic sides of the SbpA monolayer at the glass surface is crucial for the development of a tunable, facile and reliable cell patterning method. Since the assembly and orientation of S-layer proteins are dependent on the surface charge of the solid

support, the presence of bivalent ions and protein conformation, the current recrystallization procedure was originally optimized using basic conditions (pH 9.0) in the presence of Ca^{2+} ions.[44,45] To investigate self-assembly and monolayer orientation under varying buffer conditions, SbpA recrystallization was performed below and above the IEP (see also Figure 2B) to significantly change protein and glass surface properties. A single step recrystallization procedure using pH of 4.0 and 9.0 was selected to investigate SbpA nanolayer orientation. SbpA recrystallization was also performed in a two-step, layer-by-layer procedure to demonstrate the ability of SbpA monomers to form controlled double layers on solid supports (see also Figure 1). The layer-by-layer procedure consisted of recrystallization at pH 4 and then again at pH 9.0 to align the rough cytophilic sides of the monolayers with each other. Figure 3 shows the results of a comparative pH-dependent recrystallization study employing the single procedure (pH of 4.0 and 9.0) and the two-step layer-by-layer procedure. AFM results shown in Figure 3A reveal three different surface topographies that shared similar p4 nanolattice but different microstructures. While identical p4 square lattice symmetry points to ability of the SbpA protein monomers to self-assemble over a broad pH range, the different microstructures, however, indicate altered monolayer orientation. In contrast to the basic recrystallization conditions of pH 9.0 that formed smooth monolayers, SbpA protein recrystallized on glass at pH 4.0 featured a rough and highly "patchy" surface with a patch size of approximately 70−100 nm (see Figure 3B). Line scan depth profiles further confirmed the presence of smooth (0.5 ± 0.22 nm) and rough surfaces (2.2 nm ± 0.89 nm) following recrystallization under basic and acidic conditions using the single step method. Additional contact angle and zeta-potential measurements showed an increased surface wettability (contact angle of $\theta = 65 \pm 7°$) and shift in the IEP from a pH 4.6 to a more acidic IEP of pH 4.0 in the presence of the rough cytophilic SbpA monolayer, as seen in Figure 3D. These results indicate the presence of different surface charge distributions at the rough and smooth SbpA protein layers. In turn, the similar surface potential and charge of approximately −50 mV at pH 9 and +25 mV at pH 3 found for both acidic and basic recrystallization procedures can be explained by the same protein chemistry and p4 nanolattice symmetry of the two SbpA surfaces. Results of the layer-by-layer procedure (Figure 3A,B) revealed a smooth top surface (0.67 ± 0.21 nm) with underlying patchy surface features. The intermediate behavior displaying characteristics similar to smooth as well as rough SbpA monolayers indicates the establishment of a SbpA double layer. Additional AFM scratch assays shown in Figure 3B shows that the protein nanolayer thickness increased from of 9.73 ± 0.54 nm to 14.29 ± 1.03 nm, confirming the formation of a double layer using the layer-by-layer approach.

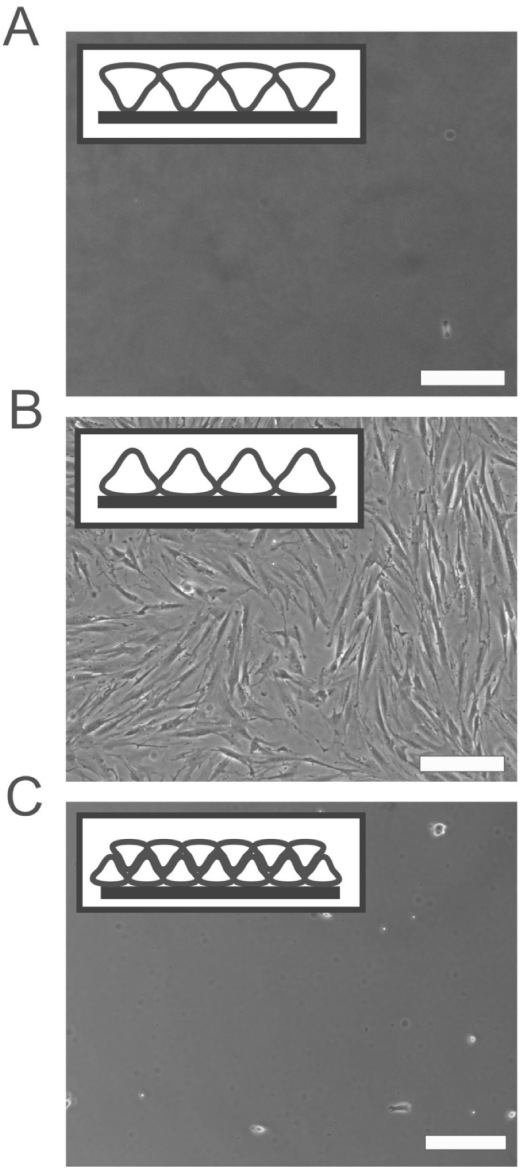

Figure 4. Light microscopic images of NHDF cells responding to the different SbpA surfaces after standard cultivation overnight: SbpA protein monolayers recrystallized at basic pH 9 (A) and at acidic pH 4 (B), and bilayer constructed layer-by-layer on glass (C). Bars, 200 μm.

To demonstrate that smooth and rough surface topographies are representative of the cytophilic inner and cytophobic outer sides of the SbpA monolayer as seen in Figure 1B, a series of cell adhesion assays were conducted. Figure 4 shows microscopic images of normal human dermal fibroblast (NHDF) cells taken after being cultured for 12 h in the presence of smooth and rough SbpA monolayers and bilayers assembled on glass. Results of this study clearly show that cell attachment and spreading took place exclusively on the crystalline rough SbpA monolayer, as seen in Figure 4B, thus, highlighting the cytophilic properties of the inner monolayer surface. However, exposure to

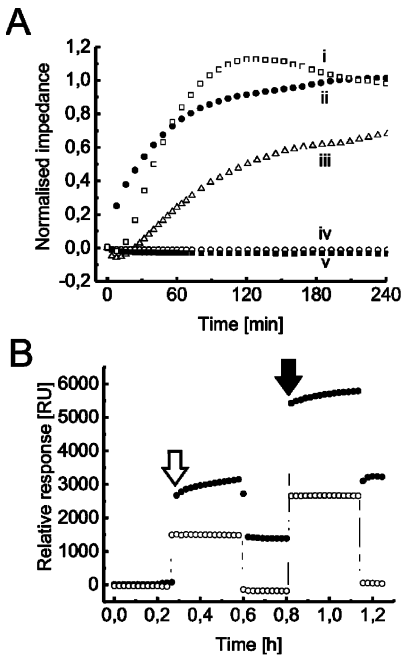

Figure 5. (A) Impedance-time traces of NHDF attachment measured at a frequency of 20 kHz: Culture medium without cells (■), smooth cytophobic (○), and rough cytophilic (●), and GRGDS-modified smooth (△) SbpA monolayers, and the unmodified ZrO_2 sensor surface (□). (B) SPR response curves of the smooth cytophobic SbpA-modified (○) and blank (●) gold sensor surface with consecutive injection of 100 μg/mL fibronectin (white arrow) and 1% gelatin solution (black arrow).

the smooth and cytophobic SbpA outer surfaces found at the monolayers and bilayers resulted in a strong inhibition of cell attachment, as shown in Figure 4A,C. These results demonstrate that the inherent SbpA anisotropy can be used to readily control cell adhesion by adjusting the orientation of SbpA monolayers. Controlled orientation of the SbpA monolayer is accomplished by simply changing the recrystallization conditions from basic to acidic pH.

Application of the Anisotropy of the S-Layer Protein SbpA for Cellular Micropatterning. The combination of our SbpA protein-based surface modification method with MIMIC was evaluated for cell patterning using a variety of mammalian cells. An important aspect of cell patterning is the biocompatibility and stability of the patterned protein monolayers. To investigate dynamic cell attachment characteristics of NHDF, standard and SbpA-modified surfaces were used in subsequent experiments. In a comparative study, EIS was employed to monitor NHDF cell adhesion on rough, smooth, and GRGDS-modified smooth SbpA monolayers. The synthetic GRGDS pentapeptide was selected because it resembles natural cell binding sites at the ECM and is commonly used as a cell adhesion promoter on culture surfaces. To create a uniform and homogeneous surface for SbpA crystallization that is also biocompatible for cell culture applications, a thin (15 nm) insulating layer of zirconia (ZrO_2) was deposited over the impedance microelectrodes.[46] AFM measurements confirmed similar p4 nanolattice symmetry for SbpA monolayers recrystallized on ZrO_2 surfaces (data not shown). Figure 5A shows the impedance-time traces of dynamic cell−substrate interactions in the initial cell adhesion process in the presences of native and modified ZrO_2 surfaces. Similar fibroblast cell adhesion dynamics were found between the native ZrO_2 surfaces (i) and the rough, cytophilic SbpA monolayer (ii), thus, indicating unchanged and unaffected cellular activity in the presence of the bacterial SbpA protein. Visual inspection (phase contrast microscopy) after 14 h of cell attachment and proliferation confirmed high cell viability and stable SbpA monolayers. While the GRGDS-modified smooth SbpA monolayer (iii) showed cell adhesion and 100% cell coverage after 10 h in culture, a significant delay in cell attachment was observed. These results indicate that the underlying cytophobic properties of the smooth SbpA-monolayer may affect initial NHDF cell attachment. In contrast, the smooth and cytophobic SbpA monolayer showed no measurable cell attachment and was similar to the negative control without cells as seen in traces (iv) and (v) of Figure 5A.

To further study the cytophobic characteristic of the smooth SbpA monolayer surface, SPR was performed to assess protein adsorption at the SbpA monolayer, which is also known to influence cell adhesion. Fibronectin and gelatin, two well-known protein-based cell adhesion promoters, were used as model to mimic the establishment of the ECM at the SbpA monolayer. These fibrous proteins play a major role in the regulation of cell adhesion and thus tissue development.[47] Smooth SbpA monolayers were recrystallized on SCWP-modified gold surfaces at pH 9.0 followed by two consecutive injections of fibronectin and gelatin. Figure 5B shows a significant mass increase of 1.31 and 1.78 ng/mm^2 for fibronectin and gelatin adsorption at the unmodified gold surface. In turn, the presence of the smooth SbpA-monolayer effectively inhibited protein adsorption, resulting in a marginal mass increase of less than 0.21 ng/mm^2. Similar observations were also found using human plasma and whole blood samples where smooth SbpA monolayers were employed as antifouling layers in microfluidic devices.[48] The effective elimination of protein adsorption is an important aspect of cell patterning methods because different cancer and primary mammalian cells are able to degrade protein patterns and remodel their extracellular environment. The resulting breakdown of protein surfaces due to localized enzymatic digestion frequently leads to applied surface patterns that fail.[49]

Because the unique cytophobic and cytophilic characteristics of the SbpA layer are ideally suited for simple and reliable cell patterning, a practical approach is demonstrated using fibroblastoid mammalian cell cultures including smooth muscle cells (SMC) and NHDF

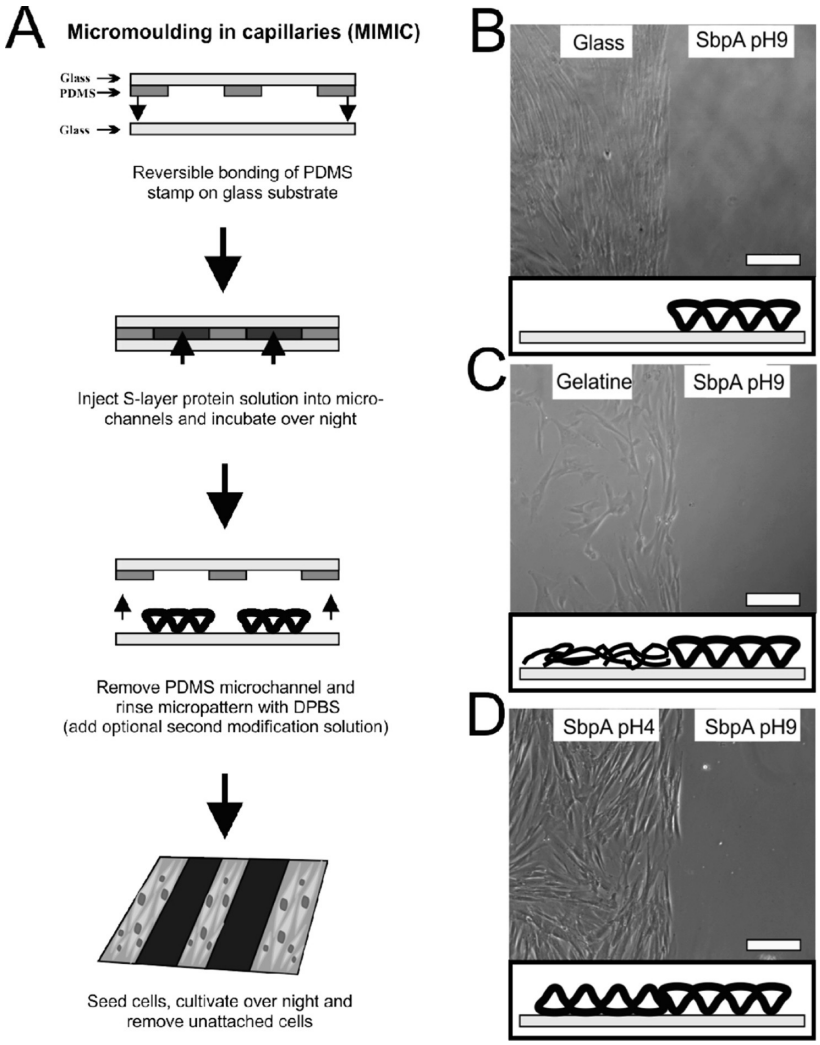

Figure 6. (A) Schematic illustration of the MIMIC patterning procedure on glass using PDMS microchannels. (B) Light microscopic image of NHDF cells cultured on smooth SbpA patterns. (C) Light microscopic image of SMC cells cultured on smooth SbpA patterns with the untreated surface being modified with gelatin. (D) Light microscopic image of NHDF cells cultured on smooth and rough pH 4 and 9 SbpA patterns. Bars, 200 μm.

cells. While the controlled orientation of the smooth and rough SbpA layers was realized by pH-dependent recrystallization, the spatial alignment of the cytophilic and cytophobic SbpA layers was accomplished by MIMIC. Figure 6A shows a schematic layout of the MIMIC surface structuring procedure employed in the evaluation of our SbpA-based cell patterning method. The ability of smooth SbpA patterns to effectively abolish cell adhesion was demonstrated for spatial patterning of NHDF cells, as seen in Figure 6B. Further, the elimination of unwanted protein adsorption allows for rapid, facile and selective functionalization of the unmodified and unpatterned regions using standard protein-based cell adhesion promoters. Thus, the cell culture performance of our SbpA protein patterns can be advanced as demonstrated for the cultivation of SMCs on SbpA surface patterns where the untreated surface area was modified with gelatin (see Figure 6C). The performance of our micropatterns was additionally evaluated for HeLa, CaCo-2, and HUVEC cell cultures and regardless of cell morphology, no cell attachment was found on the smooth, cytophobic SbpA surface (data not shown). Long-term studies further demonstrated the inherent resistance of the patterned smooth and cytophobic SbpA layer to cell-induced remodeling processes. For instance, a continuous cell culture using NHDF showed that the time-to-failure of our SbpA patterns is over 30 days (data not shown).

To finally demonstrate the ability of our SbpA-based cell patterning method to create a single protein coating that features cytophilic and cytophobic areas, a two-step SbpA patterning approach was established. MIMIC was employed in the first step to pattern smooth, cytophobic SbpA layer on top of glass. This was followed by the removal of the MIMIC and a recrystallization procedure to generate a rough, cytophilic SbpA layer at the remaining unmodified surface area. Figure 6D shows NHDF cell adhesion after

overnight cell culture and demonstrates the clear spatial separation between the smooth, cytophobic and rough, cytophilic SbpA moieties. These results demonstrate that the pH-dependent anisotropy of SbpA monolayers can be exploited to readily generate reliable and stable cell patterns based on a single protein material.

CONCLUSION

We have developed a rapid, facile, and reliable cell patterning method involving protein self-assembly and controlled monolayer orientation combined with MIMIC technology. Our protein-based strategy exploits the inherent anisotropic properties of the S-layer protein SbpA isolated from the Gram-positive mesophilic *Lysinibacillus sphaericus* CCM 2177 strain that features, depending on its orientation, either a rough cytophilic or a smooth cytophobic surface. By simply altering the recrystallization protocol from basic to acidic conditions, the SbpA-protein layer orientation can be adjusted to effectively prevent protein adsorption and cell adhesion or to promote cell attachment and spreading. Due to charge asymmetries of the S-layer protein subunits, recrystallization of SbpA at acidic pH (<IEP) results in the formation of cell-attractive (cytophilic) surface regions where the protein's inner rough side is oriented toward the cell-medium-interface. We believe that the self-assembly mechanism at pH 4 is related to the strong electrostatic interaction between the SbpA subunits and the negatively charged glass surface. In contrast, recrystallization of SbpA at pH 9.0 in the presence of 10 mM $CaCl_2$ forms long-range and ordered growing crystals of 100−150 nm in size because ion bridging between the S-protein subunits and glass occurs in the presence of bivalent ions such as Ca^{2+} and Mg^{2+}.[50,51]

It is important to mention that, in the presence of the rough cytophilic orientation of the SbpA layer, no additional surface functionalization using common adhesion-promoters, such as fibronectin or gelatin, were needed to induce strong adhesion preference in a variety of mammalian cells. However, our S-layer protein cell patterning method is still compatible with standard surface modification procedures due to the effective elimination of protein adsorption in the presence of the smooth cytophobic SbpA monolayer. The inherent resistance to enzymatic digestions and biodegradation makes smooth SbpA patterned regions stable for over 30 days in cell culture by preventing cell-induced remodeling of its environment. S-layer stability constitutes a major advantage over existing protein-based cell patterning methods where cellular degradation leads to the breakdown of, for example, agarose, pluronics, and BSA patterned surfaces, thus, severely limiting their long-term application.[52] Although in a previous study patterns of poly-L-lysine grafted polyethylene glycol and smooth SbpA monolayers were fabricated using μCP technology,[53] the generation of two chemically and topographic different materials on a single substrate may induce cell orientation and alignment along the micrometer-sized height divergences, thus, altering cell phenotypes. In turn, the establishment of cytophobic and cytophilic SbpA layers makes possible the generation of surface patterns with uniform height (9−10 nm), identical p4 lattice symmetry, as well as similar surface potential and charge distributions. The pH-dependent protein "orientation switch" was integrated using MIMIC to rapidly generate the spatial patterning of cytophilic and cytophobic regions using a single protein solution.

METHODS

Cell Culture. Normal human dermal fibroblasts (NHDF), smooth muscle cells (SMC), HeLa, and HepG2, as well as Caco-2 epithelial cells, were cultivated in MEM medium (PAA, Austria) supplemented with 10% fetal bovine serum (FBS, PAA, Austria), 1% L-glutamine (PAA, Austria), and 1% antibiotic/antimycotic mix (PAA, Austria) under standard cell culture conditions at 37 °C in 5% CO_2 humidified atmosphere as adherent monolayers in 25 cm^2 cell culture flasks (Iwaki, Japan). Human umbilical vein endothelial cells (HUVEC) were maintained using EndoPrime medium kit (PAA, Austria) supplemented with 2% EndoPrime FBS and 5% EndoPrime human serum. Upon reaching confluence, cells were split using 0.25% trypsin EDTA (PAA, Austria) at 37 °C for enzymatic detachment. For cultivation of SMC and HUVEC all culture vessels were precoated with 1% gelatin solution (gelatin from cold water fish skin, Sigma Aldrich, Austria) for 10 min at 37 °C. Cells were routinely split 1:2 to 1:6 once to twice a week.

Isolation and Recrystallization Procedures of S-Layer Protein SbpA onto Planar Supports. The isolation of S-layer protein SbpA of *Lysinibacillus sphaericus* CCM 2177 is in detail described elsewhere.[54] Recrystallization of SbpA proteins on glass substrates the S-layer protein solution was prepared using 2 mg lyophilized protein dissolved in 5 M GHCl in 50 mM Tris-(hydroxymethyl)-aminomethane hydrochloride buffer pH 7.2 and dialyzed against Milli-Q water (Millipore, Germany) for 1 h at 4 °C with water exchange after 30 min. After dialysis the protein solution was centrifuged at 13000 rpm for 15 min at 4 °C to remove protein aggregates. The protein concentration of the solution was measured using a NanoDrop spectrophotometer (ND-1000, Wilmington, U.S.A.) at 280 nm with the respective extinction coefficient of 85150 and molecular weight of 129091 Da. Prior recrystallization the protein solution was adjusted to 100 μg/mL in 0.5 mM Tris-HCl buffer pH 9.0 containing 10 mM $CaCl_2$, deposited on cleaned glass substrates, and incubated overnight at room temperature.

Transmission Electron Microscopy. Epithelial HepG2 cells were grown to 60−70% confluence on glass slides (Ø 13 mm) before incubated with nonassembled as well as self-assembled SbpA protein in solution (1 mg/mL) and cultured under standard cell culture conditions for 12 h in 5% CO_2 humidified atmosphere. For electron microscope study cell monolayers were subjected to ultrathin sectioning as described in literature.[55]

Topographic and Physicochemical Characterization. S-layer proteins recrystallized on glass cover slides (Ø 13 mm) were analyzed using Nanoscope IIIa atomic force microscope (Veeco Instruments, U.S.A.) in contact mode. Silicon nitride NP-S10 cantilevers (NanoProbes, Digital Instruments) with a nominal spring constant of 0.58 N/m were used. The sample surface was scanned at 2−4 Hz on areas ranging from 10 μm down to 500 nm and the applied force during scanning was minimized to prevent the tip from manipulation of the sample. Samples

were measured in 0.1 M NaCl solution to avoid electrostatic interactions between sample and tip. For all scratching experiments a 0.25 μm^2 area was scratched into the protein layer at a scan speed of 30 Hz at constant load (3 V higher load) and for statistical analysis six line scans were performed per sample. For S-layer surface profile determination 10 line scans in scan direction of a scan area of 0.25 μm^2 were analyzed using the manufacturer's software (Nanoscope application, version 7.3).

The zeta potential of the crystalline S-layer samples was determined by streaming potential measurements using an adjustable gap cell for 10 × 20 mm rectangular substrates in an electrokinetic analyzer (SurPASS, Anton Paar GmbH, Austria). The gap height of the fluidic channel formed by two planar samples was adjusted to 100 μm and the streaming potential was sensed by two Ag/AgCl electrodes. A background electrolyte of 1 mM KCl solution was used and 0.1 M HCl and 0.1 M NaOH was used to adjust the pH in the range of 3.0 to 9.0. The zeta potential was determined from the measured streaming potential based on Fairbrother-Mastin.[56]

The contact angle measurements of water droplets deposited on glass substrates of that have been modified with crystalline S-layer proteins was conducted using a goniometer (Easy Drop DSA15, Krüss, Germany). Data were analyzed with the enclosed manufacturer's software (DSA software, version 1.91.0.2). First, the S-layer coated surface was dried under a stream of nitrogen and under vacuum overnight. After deposition of 2 μL droplet of Milli-Q water on the surface the contact angle was recorded for 10 min.

SbpA Protein Modification Using GRGDS Peptide. The synthetic pentapeptide sequence of GRGDS (Gly-Arg-Gly-Asp-Ser) known to mimic the cellular binding site of a variety of adhesive ECM proteins was immobilized onto S-layer protein SbpA. Following initial crystallization the SbpA monolayer was allowed to cross-link for 30 min at room temperature using a 2.5% glutaraldehyde solution (Grade I, 50% in H_2O, Sigma-Aldrich, St. Louis, MA) in 0.2 M sodium cacodylate buffer pH 7.2. Next, activation of the S-layer was achieved by addition of 0.1 M 1-ethyl-3-(3-dimethylaminopropyl)carbodiimide (Sigma-Aldrich, St. Louis, MO) in 10 mM 2-(*N*-morpholino)ethanesulfonic acid (MES, Gerbu, Germany) buffer at pH 4.75. A 0.1 M GRGDS peptide solution in MES buffer was then applied to immobilize the peptide on preactivated carboxyl groups of SbpA and incubated for 2 h at room temperature.

Cell–Substrate Interaction Assay Using Electric Impedance Spectroscopy. An in-house built impedance spectroscopy platform allowing 12 parallel measurements was used for electric impedance spectroscopy. The core of the system was an integrated impedance converter AD5933 (Analog Devices, Austria). Control of the impedance converter and data recording was performed with LabView (version 8.5). To enable measurement of small impedances additional circuit consisted of the AD8531 was implemented to attenuate the excitation signal from 200 mV to 48 mV (peak to peak). All measurements were performed at 20 kHz. Biochips containing four interdigitated microsensors containing 38 individual fingers of 1.5 mm length and 15 μm width that are separated by 15 μm gap were manufactured using lithographic processes described elsewhere.[57] A unique feature of the employed parallel impedance analyzer is that the embedded impedance microsensors of each biochip were covered with a 15 nm ZrO_2 passivation layer using atomic layer deposition technique to realize a uniform and biocompatible solid interface for controlled S-layer assembly and cell adhesion. Prior cell seeding, the microsensors were modified with S-layer protein solutions, as described above. EIS measurements were conducted using a NHDF cells seeding density of 120% confluence to ensuring uniform cell density between measurements.

Protein Adsorption Assay Using Surface Plasmon Resonance Spectroscopy. Surface plasmon resonance was performed on a BIACORE 2000 instrument (Biacore International AB, Germany) with SPR gold sensor chips (Ssens bv, Netherland). The running buffer was degassed Milli-Q water. Buffer flow rate was 2 μL/min if not indicated differently. For generation of S-layer protein monolayers on the sensor chip the thiolated SCWP for SbpA was attached to the surface as anchor molecule for the S-layer protein subunits as previously described.[58] Protein solution of SbpA was injected for 60 min at a concentration of 100 $\mu g/\mu L$ in crystallization buffer at a flow rate of 2 μL/min allowing S-layer protein assembly followed by rinsing at a flow rate of 3 μL/min to remove nonbound protein subunits. For protein adsorption experiments 100 μg/mL fibronectin and 1% gelatin solution in Dulbecco's phosphate buffer saline was injected sequentially for 12 min at a flow rate of 3 μL/min, followed by a rinsing step with running buffer.

Fabrication of the Micromolding in Capillaries Device. Fabrication of the MIMIC device was accomplished by cutting four 1 mm broad polydimethylsiloxane (PDMS) stripes of 1 mm height (Sylgard 184, Dow Corning, U.S.A.), aligned on a 20 × 10 mm glass substrate (Menzel, Germany), and irreversibly bonded by plasma treatment using an easiGlow system (Pelco, U.S.A.). The PDMS devices and 20 × 20 mm glass cover slides (Menzel, Germany), which were cleaned with 70% ethanol and Milli-Q water, and sterilized at 180 °C for 2 h. Next, the mold was reversibly pressed onto the substrates and the protein coating solution was injected into the microchannels. To generate single-protein-patterns the S-layer protein solution was allowed to crystallize overnight at room temperature. Following removal of the PDMS-based micromolding device the patterned substrates were stored in sterile Milli-Q water until cell culture application. To generate the dual-protein layer-patterns a secondary incubation step was introduced to allow for an additional protein self-assembly to coat the initial uncoated glass surface.

Conflict of Interest: The authors declare no competing financial interest.

Acknowledgment. The authors would like to thank J.-L. Tocca-Herrera and J. Friedman for their assistance in AFM-imaging (Institute of Biophysics of the University of Life Sciences Vienna). The authors would also like to acknowledge O. Bethge, Vienna University of Technology, for the zirconium dioxide deposition of EIS microchips at the ZMNS, Zentrum für Mikro- und Nanostrukturen. Financial support received from the Center of Innovation and Technology (ZIT), Vienna, Austria, is greatly acknowledged. Microfabrication was carried out in the clean rooms of the CTFT, Center of Thin Film Technology of the AIT.

REFERENCES AND NOTES

1. Thery, M. Micropatterning as a Tool to Decipher Cell Morphogenesis and Functions. *J. Cell Sci.* **2010**, *123*, 4201–4213.
2. Proksch, S.; Steinberg, T.; Schulz, S.; Sauerbier, S.; Hellwig, E.; Tomakidi, P. Environmental Biomechanics Substantiated by Defined Pillar Micropatterns Govern Behavior of Human Mesenchymal Stem Cells. *Cell Transplant.* **2012**, *21*, 2455–2469.
3. Kolind, K.; Leong, K. W.; Besenbacher, F.; Foss, M. Guidance of Stem Cell Fate on 2D Patterned Surfaces. *Biomaterials* **2012**, *33*, 6626–6633.
4. Flemming, R. G.; Murphy, C. J.; Abrams, G. A.; Goodman, S. L.; Nealey, P. F. Effects of Synthetic Micro- and Nano-Structured Surfaces on Cell Behavior. *Biomaterials* **1999**, *20*, 573–588.
5. Hwang, C. M.; Park, Y.; Park, J. Y.; Lee, K.; Sun, K.; Khademhosseini, A.; Lee, S. H. Controlled Cellular Orientation on PLGA Microfibers with Defined Diameters. *Biomed. Microdev.* **2009**, *11*, 739–746.
6. Shang, S.; Yang, F.; Cheng, X.; Walboomers, X. F.; Jansen, J. A. The Effect of Electrospun Fibre Alignment on the Behaviour of Rat Periodontal Ligament Cells. *Euro. Cells Mater.* **2010**, *19*, 180–192.
7. Oakley, C.; Brunette, D. M. The Sequence of Alignment of Microtubules, Focal Contacts and Actin-Filaments in Fibroblasts Spreading on Smooth and Grooved Titanium Substrata. *J. Cell Sci.* **1993**, *106*, 343–344.
8. den Barber, E. T.; de Ruijter, J. E.; Ginsel, L. A.; von Recum, A. F.; Jansen, J. A. Orientation of ECM Protein Deposition, Fibroblast Cytoskeleton, and Attachment Complex Components on Silicone Microgrooved Surfaces. *Biomed. Mater. Res.* **1998**, *40*, 291–300.

9. Teixeira, A. I.; Abrams, G. A.; Bertics, P. J.; Murphy, C. J.; Nealey, P. F. Epithelial Contact Guidance on Well-Defined Micro- and Nanostructured Substrates. *J. Cell Sci.* **2003**, *116*, 1881–1892.
10. Yamazoe, H.; Uemura, T.; Tanabe, T. Facile Cell Patterning on an Albumin-Coated Surface. *Langmuir* **2008**, *24*, 8402–8404.
11. Tourovskaia, A.; Barber, T.; Bronwyn, T. W.; Hirdes, D.; Grin, B.; Castner, D. G.; Healy, K. E.; Folch, A. Micropatterns of Chemisorbed Cell Adhesion-Repellent Films Using Oxygen Plasma Etching and Elastomeric Masks. *Langmuir* **2003**, *19*, 4754–4764.
12. Chen, C. S.; Mrksich, M.; Huang, S.; Whitesides, G. M.; Ingber, D. E. Micropatterned Surfaces for Control of Cell Shape, Position, and Function. *Biotechnol. Prog.* **1998**, *14*, 356–363.
13. Folch, A.; Ayon, A.; Hurtado, O.; Schmidt, M. A.; Toner, M. Molding of Deep Polydimethylsiloxane Microstructures for Microfluidics and Biological Applications. *J. Biomech. Eng.* **1999**, *121*, 28–34.
14. Yap, F. L.; Zhang, Y. Protein and Cell Micropatterning and its Integration with Micro/Nanoparticles Assembly. *Biosens. Bioelectron.* **2007**, *22*, 775–788.
15. Jang, M. J.; Nam, Y. Aqueous Micro-Contact Printing of Cell-Adhesive Biomolecules for Patterning Neuronal Cell Cultures. *Biochip J.* **2012**, *6*, 107–113.
16. Raghavan, S.; Desai, R. A.; Kwon, Y.; Mrksich, M.; Chen, C. S. Micropatterned Dynamically Adhesive Substrates for Cell Migration. *Langmuir* **2010**, *26*, 17733–17738.
17. Bretagnol, F.; Lejeune, M.; Papadopoulou-Bouraoui, A.; Hasiwa, M.; Rauscher, H.; Ceccone, G.; Colpo, P.; Rossi, F. Fouling and Non-Fouling Surfaces Produced by Plasma Polymerization of Ethylene Oxide Monomer. *Acta Biomater.* **2006**, *2*, 165–172.
18. Bouaidat, S.; Berendsen, C.; Thomsen, P.; Petersen, S. G.; Wolff, A.; Jonsmann, J. Micro Patterning of Cell and Protein Non-Adhesive Plasma Polymerized Coatings for Biochip Applications. *Lab Chip* **2004**, *4*, 632–637.
19. Goessl, A.; Bowen-Pope, D. F.; Hoffman, A. S. Control of Shape and Size of Vascular Smooth Muscle Cells *In Vitro* by Plasma Lithography. *Biomed. Mater. Res.* **2001**, *57*, 15–24.
20. Folch, A.; Toner, M. Microengineering of Cellular Interactions. *Annu. Rev. Biomed. Eng.* **2000**, *2*, 227–256.
21. Tan, J. L.; Liu, W.; Nelson, C. M.; Raghavan, S.; Chen, C. S. Simple Approach to Micropattern Cells on Common Culture Substrates by Tuning Substrate Wettability. *Tissue Eng.* **2004**, *10*, 865–872.
22. Mrksich, M.; Dike, L. E.; Tien, J.; Ingber, D. E.; Whitesides, G. M. Using Microcontact Printing to Pattern the Attachment of Mammalian Cells to Self-Assembled Monolayers of Alkanethiolates on Transparent Films of Gold and Silver. *Exp. Cell Res.* **1997**, *235*, 305–313.
23. Folch, A.; Toner, M. Cellular Micropatterns on Biocompatible Materials. *Biotechnol. Prog.* **1998**, *14*, 388–392.
24. Tien, J.; Chen, C. S. Patterning the Cellular Microenvironment. *IEEE Eng. Med. Biol.* **2002**, *21*, 95–98.
25. Janssen, M. I.; van Leeuwen, M. B.; Scholtmeijer, K.; van Kooten, T. G.; Dijkhuizen, L.; Wosten, H. A. Coating with Genetic Engineered Hydrophobin Promotes Growth of Fibroblasts on a Hydrophobic Solid. *Biomaterials* **2002**, *23*, 4847–4854.
26. Sleytr, U. B.; Schuster, B.; Egelseer, E. M.; Pum, D.; Horejs, C. M.; Tscheliessnig, R.; Ilk, N. Nanobiotechnology with S-Layer Proteins as Building Blocks. *Prog. Mol. Biol. Transl. Sci.* **2011**, *103*, 277–352.
27. Sleytr, U. B.; Huber, C.; Ilk, N.; Pum, D.; Schuster, B.; Egelseer, E. M. S-Layers as a Tool Kit for Nanobiotechnological Applications. *FEMS Microbiol. Lett.* **2007**, *267*, 131–144.
28. Sleytr, U. B.; Messner, P.; Pum, D.; Sara, M. Crystalline Bacterial Cell Surface Layers (S Layers): From Supramolecular Cell Structure to Biomimetics and Nanotechnology. *Angew. Chem., Int. Ed.* **1999**, *38*, 1035–1054.
29. Sára, M.; Sleytr, U. B. Production and Characteristics of Ultrafiltration Membranes with Uniform Pores from Two-Dimensional Arrays of Proteins. *J. Membr. Sci.* **1987**, *33*, 27–49.
30. Sara, M.; Egelseer, E. M.; Dekitsch, C.; Sleytr, U. B. Identification of Two Binding Domains, One for Peptidoglycan and Another for a Secondary Cell Wall Polymer, on the N-Terminal Part of the S-Layer Protein SbsB from *Bacillus stearothermophilus* PV72/p2. *J. Bacteriol.* **1998**, *180*, 6780–6783.
31. Ilk, N.; Kosma, P.; Puchberger, M.; Egelseer, E. M.; Mayer, H. F.; Sleytr, U. B.; Sara, M. Structural and Functional Analyses of the Secondary Cell Wall Polymer of *Bacillus sphaericus* CCM 2177 That Serves As an S-Layer-Specific Anchor. *J. Bacteriol.* **1999**, *181*, 7643–7646.
32. de la Fuente-Nunez, C.; Mertens, J.; Smit, J.; Hancock, R. E. The Bacterial Surface Layer Provides Protection against Antimicrobial Peptides. *Appl. Environ. Microb.* **2012**, *78*, 5452–5456.
33. Sleytr, U. B.; Messner, P. Crystalline Surface Layers in Procaryotes. *J. Bacteriol.* **1988**, *170*, 2891–2897.
34. Pum, D.; Toca-Herrera, J. L.; Sleytr, U. B. S-layer Protein Self-Assembly. *Int. J. Mol. Sci.* **2013**, *14*, 2484–2501.
35. Sleytr, U. B. Self-Assembly of the Hexagonally and Tetragonally Arranged Subunits of Bacterial Surface Layers and their Reattachment to Cell Walls. *J. Ultrastruct. Res.* **1976**, *55*, 360–377.
36. Schuster, B.; Sleytr, U. B. Nanotechnology with S-Layer Proteins. *Methods Mol. Biol.* **2013**, *996*, 153–175.
37. Sleytr, U. B.; Sára, M.; Pum, D.; Schuster, B., Crystalline Bacterial Cell Surface Layers (S-Layers): A Versatile Self-Assembly System. In *Supramolecular Polymers*, 2nd ed.; Ciferri, A., Ed.; CRC Press: Boca Ranton, FL, 2005; pp 583−616.
38. Sara, M.; Pum, D.; Sleytr, U. B. Permeability and Charge-Dependent Adsorption Properties of the S-Layer Lattice from *Bacillus coagulans* E38−66. *J. Bacteriol.* **1992**, *174*, 3487–3493.
39. Kupcu, S.; Sleytr, U. B.; Sara, M. Two-Dimensional Paracrystalline Glycoprotein S-Layers as a Novel Matrix for the Immobilization of Human IgG and Their Use As Microparticles in Immunoassays. *J. Immunol. Methods* **1996**, *196*, 73–84.
40. Kupcu, S.; Sara, M.; Sleytr, U. B. Influence of Covalent Attachment of Low-Molecular-Weight Substances on the Rejection and Adsorption Properties of Crystalline Proteinaceous Ultrafiltration Membranes. *Desalination* **1993**, *90*, 65–76.
41. Kupcu, S.; Sara, M.; Sleytr, U. B. Chemical Modification of Crystalline Ultrafiltration Membranes and Immobilization of Macromolecules. *J. Membr. Sci.* **1991**, *61*, 167–175.
42. Weigert, S.; Sara, M. Ultrafiltration Membranes Prepared from Crystalline Bacterial Cell Surface Layers as Model Systems for Studying the Influence of Surface Properties on Protein Adsorption. *J. Membr. Sci.* **1996**, *121*, 185–196.
43. Altankov, G.; Richau, K.; Groth, T. The Role of Surface Zeta Potential and Substratum Chemistry for Regulation of Dermal Fibroblasts Interaction. *Mater. Werkst* **2003**, *34*, 1120–1128.
44. Baranova, E.; Fronzes, R.; Garcia-Pino, A.; Van Gerven, N.; Papapostolou, D.; Pehau-Arnaudet, G.; Pardon, E.; Steyaert, J.; Howorka, S.; Remaut, H. SbsB Structure and Lattice Reconstruction Unveil Ca^{2+} Triggered S-Layer Assembly. *Nature* **2012**, *487*, 119–122.
45. Pum, D.; Sleytr, U. B. Anisotropic Crystal-Growth of the S-Layer of *Bacillus sphaericus* CCM-2177 at the Air/Water Interface. *Colloids Surf., A* **1995**, *102*, 99–104.
46. Manicone, P. F.; Rossi Iommetti, P.; Raffaelli, L. An Overview of Zirconia Ceramics: Basic Properties and Clinical Applications. *J. Dent.* **2007**, *35*, 819–826.
47. Frantz, C.; Stewart, K. M.; Weaver, V. M. The Extracellular Matrix at a Glance. *J. Cell Sci.* **2010**, *123*, 4195–4200.
48. Picher, M. M.; Küpcü, S.; Huang, C.; Dostalek, J.; Pum, D.; Sleytr, U. B.; Ertl, P. Nanobiotechnology Advanced Antifouling Surfaces for the Continuous Electrochemical Monitoring of Glucose in Whole Blood Using a Lab-on-a-Chip. *Lab Chip* **2013**, 1780–1789.
49. Roberts, C. J.; Chen, C.; Mrksich, M.; Martichonok, V.; Ingber, D. E.; Whitesides, G. M. Using Mixed Self-Assembled Monolayers Presenting RGD and $(EG)_3OH$ Groups to

Characterize Long-Term Attachment of Bovine Capillary Endothelial Cells to Surfaces. *J. Am. Chem. Soc.* **1998**, *120*, 6548–6555.
50. Toca-Herrera, J. L.; Krastev, R.; Bosio, V.; Kupcu, S.; Pum, D.; Fery, A.; Sara, M.; Sleytr, U. B. Recrystallization of Bacterial S-Layers on Flat Polyelectrolyte Surfaces and Hollow Polyelectrolyte Capsules. *Small* **2005**, *1*, 339–348.
51. Zafiu, C.; Trettenhahn, G.; Pum, D.; Sleytr, U. B.; Kautek, W. Electrochemical Control of Adsorption Dynamics of Surface Layer Proteins on Gold. *Phys. Chem. Chem. Phys.* **2011**, *13*, 3478–3483.
52. Nelson, C. M.; Raghavan, S.; Tan, J. L.; Chen, C. S. Degradation of Micropatterned Surfaces by Cell-Dependent and -Independent Processes. *Langmuir* **2003**, *19*, 1493–1499.
53. Saravia, V.; Kupcu, S.; Nolte, M.; Huber, C.; Pum, D.; Fery, A.; Sleytr, U. B.; Toca-Herrera, J. L. Bacterial Protein Patterning by Micro-Contact Printing of PLL-*g*-PEG. *J. Biotechnol.* **2007**, *130*, 247–252.
54. Ilk, N.; Vollenkle, C.; Egelseer, E. M.; Breitweiser, A.; Sleytr, U. B.; Sara, M. Molecular Characterization of the S-Layer Gene, SbpA, of *Bacillus sphaericus* CCM 2177 and Production of a Functional S-Layer Fusion Protein with the Ability to Recrystallize in a Defined Orientation while Presenting the Fused Allergen. *Appl. Environ. Microb.* **2002**, *68*, 3251–3260.
55. Pavelka, M.; Ellinger, A.; Debbage, P.; Loewe, C.; Vetterlein, M.; Roth, J. Endocytic Routes to the Golgi Apparatus. *Histochem. Cell Biol.* **1998**, *109*, 555–570.
56. Buksek, H.; Luxbacher, T.; Petrinic, I. Zeta Potential Determination of Polymeric Materials Using Two Differently Designed Measuring Cells of an Electrokinetic Analyzer. *Acta Chim. Slov.* **2010**, *57*, 700–706.
57. Charwat, V.; Purtscher, M.; Tedde, S. F.; Hayden, O.; Ertl, P. Standardization of Microfluidic Cell Cultures Using Integrated Organic Photodiodes and Electrode Arrays. *Lab Chip* **2013**, *13*, 785–797.
58. Vollenkle, C.; Weigert, S.; Ilk, N.; Egelseer, E.; Weber, V.; Loth, F.; Falkenhagen, D.; Sleytr, U. B.; Sara, M. Construction of a Functional S-Layer Fusion Protein Comprising an Immunoglobulin G-Binding Domain for Development of Specific Adsorbents for Extracorporeal Blood Purification. *Appl. Environ. Microb.* **2004**, *70*, 1514–1521.